

# AIRFRAME STRUCTURAL SURVIVABILITY STUDY THROUGH HYDRODYNAMIC RAM OF WELDED METALLIC WATER TANKS

**Jong Heon Kim\*, Chun Gon Kim\*\*, Seung Moon Jun\***

**\*Agency for Defense Development, Republic of Korea \*\*Korea Advanced Institute of  
Science and Technology, Republic of Korea**

## Abstract

*This paper addresses the analysis and test of the hydrodynamic ram in metallic cubic tanks with water inside. Analysis and test of hydrodynamic ram in welded metallic tanks containing water were performed to investigate the phenomena and to understand the effects on the resulting structural behavior. For a better representation of the physical phenomena, modeling of the welded edges is added to the analysis to simulate the earlier weld line fracture and its influence on the resulting hydrodynamic ram behavior. Corresponding hydrodynamic tests were performed in a modified gas gun facility, and the following panel-based examinations of engineering parameters showed that the results of the study reasonably explained the characteristics of the hydrodynamic ram.*

## 1 Introduction

This paper addresses the analysis and test of the hydrodynamic ram in metallic cubic tanks with water inside. Hydrodynamic ram is one of major man-made threats to aircraft. The effect of hydrodynamic ram is defined as the damage process that a projectile with high velocity impacts a structure with fluid inside, and then penetrates and/or detonates it to produce a blast wave [1]. Among the components of the airframe structure, fuel tanks are more vulnerable to hydrodynamic ram, and especially the wing fuel tanks are most exposed to this ballistic threat as they have large exterior areas.

For this reason, preparation of fuel tanks against hydrodynamic ram damage is required to meet the structural survivability requirement in the development of an aircraft. Besides fuel pressures exerting on the tank panels, parameters

such as fuel volatility, leakage, and joint design are also the key factors that influence the scale of the resulting structural damage. Therefore, survivability design to hydrodynamic ram is not limited to strengthening the tank material or thickness, but also includes the features such as fire suppression and advanced joint concepts, too. Foam or bladder inside the tank, advanced on board inert gas generation system (OBIGGS), and z-pinning joints are the good examples of these features.

Hydrodynamic ram is fundamentally divided into three phases: shock, drag, and cavity [1]. Entry or impact is the step that occurs before the shock phase, and the exit is the step that occurs after the cavity phase. Many previous studies identified the occurrence of each phase in hydrodynamic ram tests and properly represented it through simulations. On the other hand, structural behavior was less investigated in detail compared to the investigation of the fluid phases due to its complexity. However, hydrodynamic ram damage of the airframe component should be more realistically assessed in order to apply for the survivability design, and thus more consideration is required for the investigation. The focus of the present study is on the characteristics of this structural behavior especially during and after the structural failure.

Metallic cubic tanks containing water were used for the test and analysis of hydrodynamic ram. For panels of water tanks were welded to each other, the effect of these welded edges on the structural behavior was investigated as much as the tank material itself. Two cases of different water levels, fully filled and three quarters filled, were also studied to examine the effects of the void.

The arbitrary Lagrange-Euler coupling method was used for the analysis of the fluid-

structure interaction occurring in hydrodynamic ram, and the result was correlated with the test. Panel based examinations of various engineering parameters were performed for the purpose of the comprehensive understanding of hydrodynamic ram phenomenon.

## 2 Setup of Test and Analysis

### 2.1 Summary of Test Preparation

A cubic tank made of aluminum was used for the hydrodynamic ram test. Each side was 406 mm long and each panel was 2.28 mm thick. Panels were corner welded after installing six pressure gages inside the tank. Three of them were located along the centerline of the tank with the intention such that the locations coincide with the traveling path of the projectile, for the purpose of measuring the maximum pressures at each location. The other three were located near the tank wall in order to measure wall pressures and their influences to the structure.

Two levels of water – 100 percent and 75 percent – were applied for the test to examine the different interactions and resulting tank behavior from hydrodynamic ram. A spherical steel ball with a diameter of 19.1 mm was fired using a modified gas gun to the entry hole of the tank at 1,000 m/s for the fully filled tank and 1,019 m/s for the partially filled tank. An entry hole was initially made to guarantee the straightness of the projectile at the entry of the tank. The entry hole was covered with a Mylar film before filling the tank with water in order to prevent the water escape through the entry hole.

### 2.2 Analysis of Fluid-Structure Interaction

When there are both structure and fluid in the analysis domain, the analysis with just Lagrangian formulation that solves the structural constitutive equations of stress and strain of finite elements is not feasible. If fluid is included in the domain, it creates large deformations leading to the mesh distortion, which makes the convergence more difficult and makes the solution end up incorrect. In order to properly simulate the fluid behavior, Eulerian formulation

is required where elements are fixed in a control volume and the material flows through the mesh.

Eulerian formulation calculates the mass, momentum, and energy conservation equation, or in other words, the ALE Navier-Stokes equation [2]. Thus the final element deformation is determined after the calculation of coupling between Eulerian and Lagrangian formulations, and this ALE coupling algorithm was used in the present analysis.

LS-DYNA [3] was used for modeling and computation. After finite element modeling of the projectile, tank, water, and void as stated in 2.2, the model nodes and elements are brought into LS-DYNA pre-processor. When material data, boundary condition, and initial condition are inputted, contact between structures and coupling between structure and fluid are defined. Controlling parameters such as time step, contact and coupling parameters, hourglass, and etc. also need to be carefully used for the accuracy and convergence of explicit nonlinear solution.

### 2.3 Analysis of Welded Joints

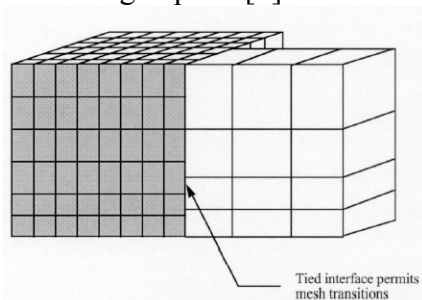
When modeling the finite elements of a structure, the interface between components such as the panel joint is typically simplified such that the panels share the nodes at the interface, or the interface is assumed to be perfectly bonded. This assumption is valid for a structure with small deformation, as the resultant deformation or strain is heavily dependent upon the overall structural material stiffness.

However, for a hydrodynamic ram case where large deformations including interface failure from ram pressure occur in a very short period, it is required to model the interfaces differently as the welded panel joints in the present case now have strong influence on the overall structure behavior. As turned out in the test result of the present case, the failure of the weld lines occurred earlier than that of the panel material, and thus, the overall displacement of each panel ends up having considerable rigid body displacement as well as the structural panel deformation. Observations of the test result that the post-test panels were severely distorted from the combination of these two different kinds of displacement support this argument. The weld

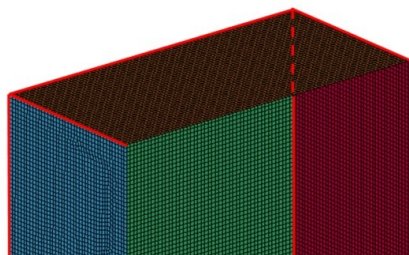
lines of the panels fail in the middle of panel bulging, and then the failing panel edges rebound at separation to produce distorted deformations. This is complex but likely in reality, where there are various interfaces consisting of airframe structures such as bonded and bolted, and welded joints between components.

The early failure of the weld line comes from the loss of the material strength. The material of the test tank was 6061-T6 aluminum alloy and it is highly weldable. The amount of strength decrease depends on the degree of heat treatment, but it is suggested that after welding the properties near the weld are typically those of annealed 6061-O which is pre-tempered and has the lowest strength among 6061 alloys [4]. The Alcoa structural handbook recommends more conservative strength if used for design [5] because the weld strength in reality varies depending on the amount of heat input, which is different for each case [6].

To add this characteristic in the analysis, weld lines between the tank panels are modeled with the tied interface of LS-DYNA [3]. The tied interface was originally developed to facilitate sudden mesh transitions, where two meshes of surface or solid elements are joined as shown in Fig. 1(a). This feature can often decrease the amount of effort required to generate meshes since it reduces the need to match nodes across interfaces of merged parts [7].



(a) Tied interface for mesh transition



(b) Weld line modeling with tied interface

Fig. 1. Modeling of tank panels with weld lines

Even though the nodes of the present tank model are not mismatched at the panel interfaces, panels do not share the nodes at the weld lines. The tiebreak contact that comes with the tied interface is useful for defining the failure criteria of the weld line separately from the panel material failure since the tiebreak contact is based on normal and shear strength failure parameters as indicated in Eq. (1). [8].

$$\left( \frac{|\sigma_n|}{NFLS} \right)^2 + \left( \frac{|\sigma_s|}{SFLS} \right)^2 \geq 1 \quad (1)$$

where  $\sigma_n (P_a)$  is the normal tensile stress,  $\sigma_s (P_a)$  is the shear stress,  $NFLS (P_a)$  is the tensile failure stress, and  $SFLS (P_a)$  is the shear failure stress. Therefore, the tiebreak contact can facilitate the modeling of connections which transmit both compressive and tensile forces with optional failure criteria. Before failure, the tiebreak contact works both in tension and compression, while after failure, the contact behaves as a surface-to-surface contact with no thickness offsets [9]. In this way, panels have separate nodes with the tiebreak interface using the property of the weld material instead of sharing the nodes at the interface even though the mesh is not visually separated. The edges of each panel are separately modeled to represent the weld line and this technique enables early joint failure occurring ahead of the panel material failures, which better represents the reality and leads to the greater agreement with the test result.

### 3 Investigation of Test and Analysis Results

#### 3.1 Pressure History

Fig. 2 displays the pressure versus time measured by three centerline and three wall gages for the fully filled tank. Two major pressure peaks were observed in the graphs of the centerline gages. The first peak indicates the arrival of the shock wave produced at the impact of the projectile, and the second peak the arrival of the projectile at the gage after the gradual pressure increase by the drag. For wall pressure there are more coupled factors affecting the pressure such as the pressure wave reflection at

the tank panels and the pressure damping by the elasticity of the tank material, which cause higher discrepancy. But overall, the analysis results follow the trend of the test data.

The differences of the peak value and the corresponding time between test and analysis are attributed to the characteristics of both test and analysis. For this kind of very short duration test and analysis with high non-linearity, there is a singularity problem especially for the centerline pressures located at the traveling path of the projectile. The sensitivity of both the test and analysis brings about the large difference by even small input changes.

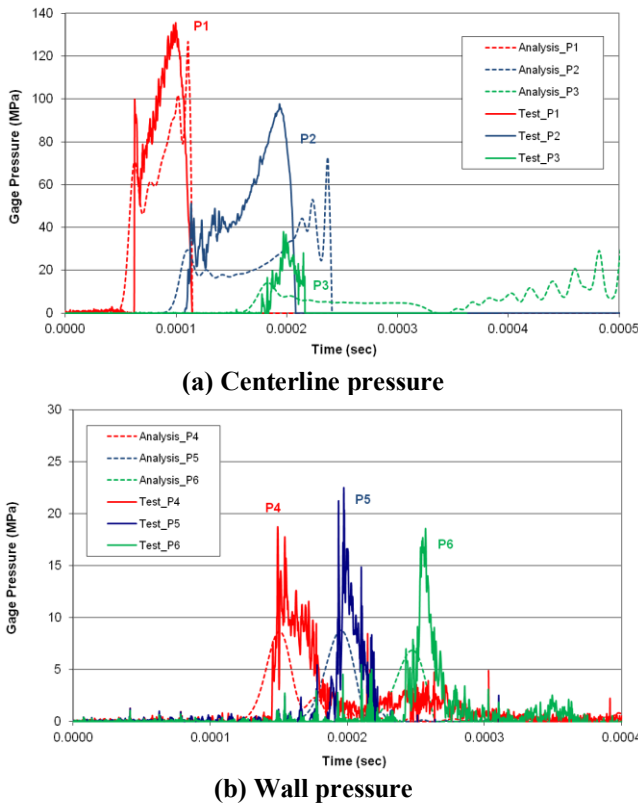


Fig. 2. Pressure history by analysis and test

The hydrodynamic ram phases are found in the pressure contour of Fig. 3(a). The highest pressure zone by the water drag is formed right at the front of the projectile, while a cavity is created behind the projectile. The large arc seen up ahead of the projectile near the exit panel signifies the shock wave traveling at the speed of sound faster than the projectile, which is one of typical phenomena of hydrodynamic ram [10]. The projectile, tank, and water of analysis result are shown together in Fig. 3(b), for the

visualization of the fluid-structure interaction after the projectile penetrates throughout the tank.

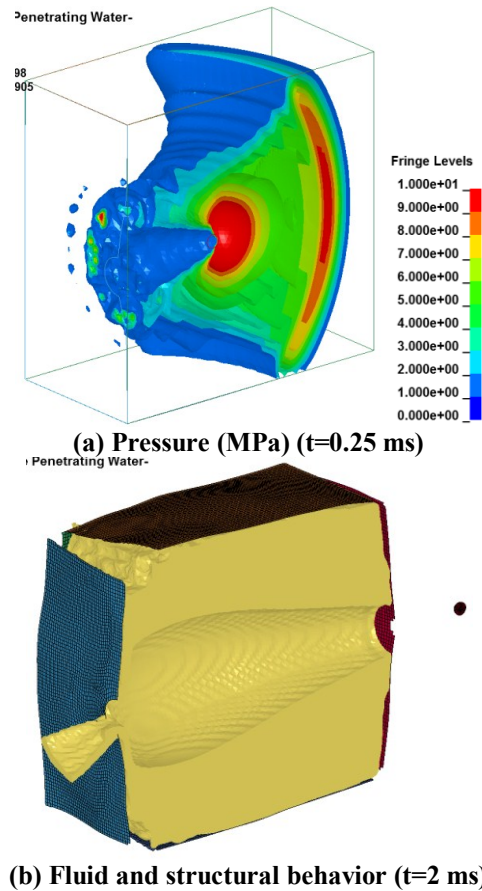
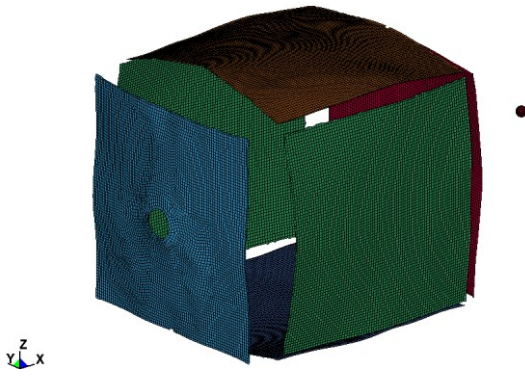


Fig. 3. Fluid pressure and interaction with structure of 100% filled tank panels by analysis

#### 4.2 Structural Deformation and Related Behaviors

The simulated structural deformation and resulting fracture of the fully filled tank are shown in Fig. 4. The combined effect of fracture at the panel edges and the bulging of the panels by hydrodynamic ram pressure produced distorted panels especially around the panel edges, which coincided with the test result shown in Fig. 5. The separated panels of the test were attached with duct tape to show the panel distortion compared to the initial state of the tank.



**Fig. 4. Structural deformation and fracture of 100% filled tank panels by analysis**

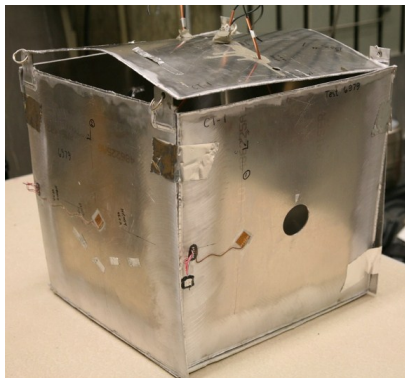
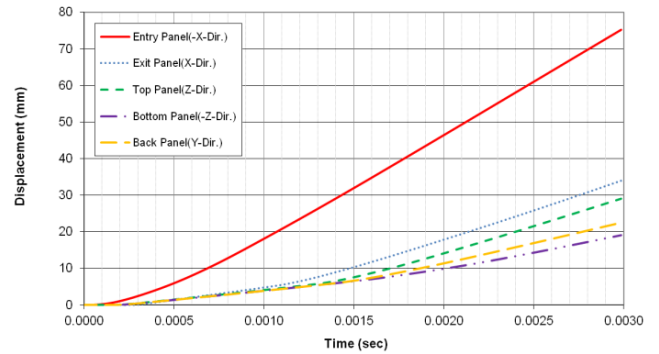


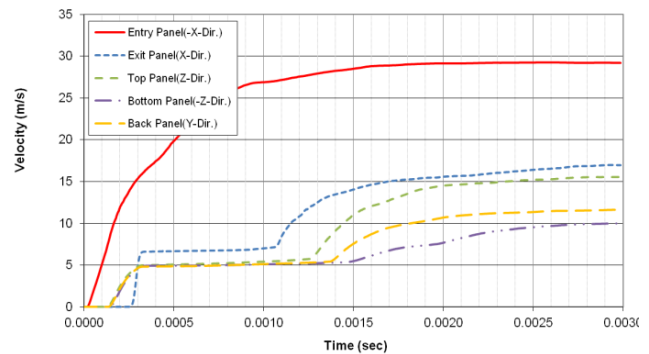
**Fig. 5. Structural deformation and fracture of 100% filled tank panels by test**

Observation of the deformation and velocity data of each panel in its moving direction at the separation enables further understanding of hydrodynamic ram. Fig. 6 shows the magnitudes of overall deformation and velocity of each panel follow are determined by how much the penetrating projectile influences the panel. Also, a closer look of the panel velocities of Fig. 6(b) explains that the velocity curves contain the phases of hydrodynamic ram that occurred during the event. Specifically for the exit panel velocity, the first small increase around 0.3 ms indicates the arrival of the shock wave, and the velocity maintains the same value after the shock wave is gone, and it increases again after 1.1 ms when the projectile reaches the exit panel and penetrates. The first velocity increases of the top, bottom, and back panels occur earlier than that of the exit panel because they are nearer to the impact location of the entry panel. However, their overall velocity magnitudes are lower than that of the exit panel as they are off the

penetrating path of the projectile from entry to exit panel.



**(a) Panel displacement**



**(b) Panel Velocity**

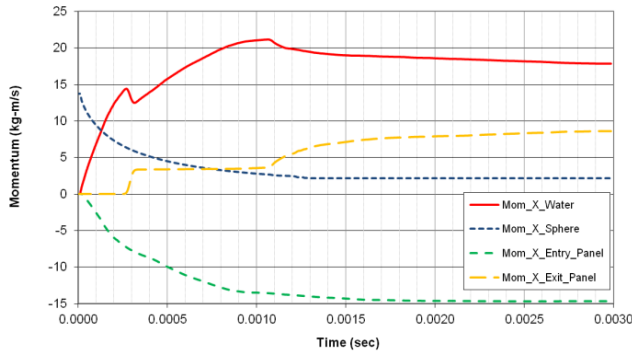
**Fig. 6. Displacement and velocity of panels for 100% filled tank by analysis**

### 4.3 Momentum and Energy

Fig. 7 illustrates the momentum of each panel to the advancing direction of the projectile versus time. Looking at the momentum of the water, the first small peak at slightly over 0.25 ms indicates the arrival of the shock pressure at the exit panel. The following small valley is produced by the shock pressure completely escaping the exit panel and disappearing. After the shock pressure, the momentum is gradually increased by the traveling projectile pushing the water toward the advancing direction. However, the momentum starts to decrease after 1 ms because the early failure and separation of the entry panel allow the escape and transfer of the water into the opposite direction, and this opposite momentum overcomes the previous increasing momentum to finally build the later part of the curve.

On the other hand the momenta of the panels are mostly attributed to rigid body motions built up since the time they are

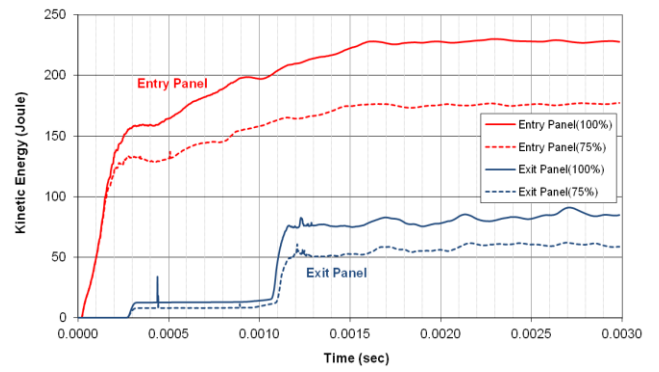
completely failed and separated, and this effect makes the momenta decrease slowly and almost stay at certain values since the time of separation.



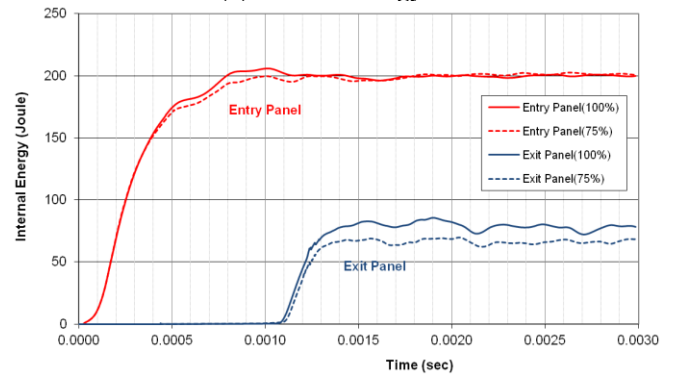
**Fig. 7. Momenta of water and panels for 100% filled tank**

Fig. 8 illustrates the kinetic and internal energies of the panels. The data of the entry and exit panels are displayed only for visual clarity. As seen in Fig. 8(a), the kinetic energy of the partially filled tank is lower than that of the fully filled tank because the amount of water, transferring the energy, is less for the partially filled tank. Even though it is not illustrated in the figure, the difference the water level makes to the kinetic energy is clearer when investigating the top and bottom panels, since the kinetic energy of the bottom panel is not much different regardless of the water level while the energy of the top panel is quite different depending on whether the upper void exists or not.

Meanwhile, the internal energy of the panels, which signifies how much the panels are deformed, is not very much affected by the water level like the kinetic energy as shown in Fig. 8(b). As compared in the two figures, the entry and exit panels of the partially filled tank are less distorted from less water, but are more bulged because the void delays the separation of the panels. These two factors end up building up no less than overall deformations and thus creating the similar energy curve in Fig. 8(b).



**(a) Kinetic energy**



**(b) Internal energy**

**Fig. 8. Energy of panels for 100% and 75% filled tanks**

#### 4 Conclusion

The hydrodynamic ram of welded metallic cubic tanks with water inside was investigated through test and analysis. Two cases of different water levels, fully filled and three quarters filled, were studied to examine the effects of the void.

The arbitrary Lagrange-Euler coupling method was applied for the analysis of the fluid-structure interaction occurring in hydrodynamic ram, where the projectile, tank, and water are exchanging load, momentum, and energy during the traveling of the projectile through the water of the tank. For the better representation of the physical phenomenon, the modeling of the welded edges is added to the analysis in order to simulate the earlier weld line fracture and its influence on the resulting hydrodynamic ram behavior.

Panel based examinations of various parameters such as displacement, velocity, stress, momentum, and energy were performed, and it showed that the analysis and test were well correlated, and thus the result of the study

reasonably explained the characteristics of hydrodynamic ram.

The results showed that the welded joints between tank panels were decisively influencing the deformation and failure progress of the tanks. This suggests that the resultant structural damage shape and scale from hydrodynamic ram in reality are highly dependent upon joint mechanism as much as the ram pressures. Therefore the ideas for uniform structural robustness against hydrodynamic ram loading are pursued for survivability design.

have obtained permission, from the copyright holder of any third party material included in this paper, to publish it as part of their paper. The authors confirm that they give permission, or have obtained permission from the copyright holder of this paper, for the publication and distribution of this paper as part of the ICAS proceedings or as individual off-prints from the proceedings.

## References

- [1] Ball, R., The Fundamentals of Aircraft Combat Survivability Analysis and Design, AIAA, 2003.
- [2] Aquelet, N., Souli, M., and Olovsson, L., “Euler–Lagrange Coupling with Damping Effects: Application to Slamming Problems”, Computer Methods in Applied Mechanics and Engineering, 2005.
- [3] LS-DYNA version 971, Livermore Software Technology Corporation (LSTC), 2007.
- [4] 6061 Aluminum Alloy. Available from: [http://en.wikipedia.org/wiki/6061\\_aluminium\\_alloy#Welding](http://en.wikipedia.org/wiki/6061_aluminium_alloy#Welding).
- [5] Alcoa Mill Products, Alcoa Structural Handbook, 2006.
- [6] “Guide for Aluminum Welding”, Maxal International Inc., 2012, pp. 6-7.
- [7] Hallquist, J., LS-DYNA Keyword User’s Manual Version 971, Livermore Software Technology Corporation (LSTC), 2007.
- [8] McCallum, S., Locking, P., and Harkness, S., “Simulation of Masonry Wall Failure and Debris Scatter”, 6th European LS-DYNA Users’ Conference, 2007.
- [9] Dolce, F., Meo, M., Wright, A., and French, M., “Structural Response of Laminated Composite Plates to Blast Load”, 17th International Conference on Composite Materials, Piscataway NJ, 2009.
- [10] Disimile, P., Swanson, L., and Toy, N., “The Hydrodynamic Ram Pressure Generated by Spherical Projectiles”, International Journal of Impact Engineering, 2009, pp. 821-829.

## 5 Contact Author Email Address

mailto:ian1973@naver.com

## Copyright Statement

The authors confirm that they, and/or their company or organization, hold copyright on all of the original material included in this paper. The authors also confirm that they